

**A gated strategy stabilizes room-temperature phosphorescence**

Kaizhi Gu, Zhengong Meng, Xing Wang Liu, Yue Wu,\* Xin Qi, Yiran Ren, Zhen-Qiang Yu,\* and Ben Zhong Tang\*

K. Gu, Z. Meng, X. W. Liu, Y. Wu, X. Qi, Y. Ren, Z. Q. Yu  
College of Chemistry and Environmental Engineering, Shenzhen University, Shenzhen 518071, China  
E-mail: [wuyue@szu.edu.cn](mailto:wuyue@szu.edu.cn); [zqyu@szu.edu.cn](mailto:zqyu@szu.edu.cn)

K. Gu  
Institute for Advanced Study, Central South University, Changsha, Hunan 410083, China

B. Z. Tang  
School of Science and Engineering, Shenzhen Institute of Aggregate Science and Technology, The Chinese University of Hong Kong, Shenzhen 518172, China  
E-mail: [tangbenz@cuhk.edu.cn](mailto:tangbenz@cuhk.edu.cn)

Keywords: room-temperature phosphorescence, gated effect, grinding, protonation, molecular packing

**Abstract:**

Room-temperature phosphorescence (RTP) of purely organic materials is easily quenched with unexpected purposes because the excited triplet state is extremely susceptible to external stimuli. How to stabilize the RTP property of purely organic luminogens is still challenging and considered as the bottleneck in the further advancement of the bottom-up approach. Here, we describe a gated strategy that can effectively harness RTP by employing complexation/dissociation with proton. Due to the order-disorder transition orientation of intermolecular packing, the RTP of triazine derivative Br-TRZ will easily vanish upon mechanical force. Impressively, by enhancing its intramolecular charge transfer effect, the protonated Br-TRZ stubbornly possesses an obvious RTP under external grinding, whatever in the ordered or disordered intermolecular arrangement state. Consequently, the “Lock” gate of RTP was achieved in the protonated Br-TRZ molecule. Combined with theoretical calculation analysis, the enhanced charge transfer effect can narrow the singlet–triplet energy gap significantly, and stabilize the RTP property of triazine derivative sequentially.

Furthermore, the locked RTP can be tuned via proton and counterions repeatedly and show excellent reversibility. This gated RTP concept provide an effective strategy for stabilizing the RTP emission of purely organic systems.

## 1. Introduction

Room-temperature phosphorescence (RTP), a unique photophysical phenomenon that originates from the radiative transition from the lowest triplet excited state to the ground state, has attracted great interest because of their potential for bioimaging, information anti-counterfeiting, organic light-emitting diodes (OLED), and so on.<sup>[1–7]</sup> However, for a long time, the RTP emission has long been considered the exclusive feature of traditional inorganic materials or metal complexes, which suffer from high cost, potential toxicity, and instability in aqueous environments.<sup>[8–12]</sup> As compared to metal-containing luminophores, the pure organic molecules with bright and persistent RTP are really scarce because the intersystem crossing (ISC) between singlet and triplet state is inherently inefficient and the highly active triplet excitons are exhausted fast by non-radiative transition and quenchers such as oxygen.<sup>[13–18]</sup> Therefore, the development of high-performance purely organic RTP luminogens is of great significance.

In principle, the key step to obtaining robust RTP from organic molecules is the promotion of ISC efficiency, which is usually low compared to inorganic counterparts. Fortunately, several different strategies, including crystal or non-covalent co-crystals engineering,<sup>[19–23]</sup> host-guest doping,<sup>[24–26]</sup> polymerization,<sup>[27–29]</sup> and others<sup>[30–32]</sup> have been proposed to improve ISC process, especially stabilize the triplet excitons under ambient to achieve high-performance organic RTP materials. Given that the excited triplet state of phosphors is extremely susceptible to external stimuli such as force, heat, light, etc., purely organic RTP is easily eliminated with unexpected purposes.<sup>[33–38]</sup> It is thus emerging to circumvent this

bottleneck in the development of enhancing and stabilizing RTP strategy by providing a straightforward and general route to steady RTP materials.

With this in mind, we firstly employ a gated phosphorescence concept, which can offer additional protection from the external interference to perform organic RTP. Taking advantage of the nucleophilicity of available triazine derivative, herein, we explore the unique proton binding ability to design proton specifically gated RTP for organic materials bromine-substituted triazine (Br-TRZ in Figure 1), whose RTP property could be triggered by thermal annealing.<sup>[39,40]</sup> However, the annealing-induced RTP of Br-TRZ will vanish after external stimuli such as mechanical grinding. Upon addition of trifluoroacetic acid (TFA), the intramolecular charge transfer (CT) effect of protonated Br-TRZ (Br-TRZ-H) has been enhanced greatly, resulting in the emergence of highly emissive RTP. Different from the thermal annealing, the proton-bonding Br-TRZ-H still exhibits strong RTP emission after grinding. The gated RTP will vanish just in the condition of triethylamine (TEA) fuming. Thus the RTP property of the triazine derivative can be regulated by acid/base in a “*Lock-and-Unlock*” manner, with the following features: (i) efficient RTP trigger via protonation, (ii) high fatigue resistance in the gated RTP, (iii) stabilized RTP property while undergoing mechanical force. This gated RTP concept by the enhanced charge transfer effect describes a practicable and efficient strategy to stabilize organic RTP emission.

## 2. Results and discussion

In triazine-derivative compound Br-TRZ, electron donor of diphenyl and electron acceptor of triazine are connected by covalent bond. We first investigated the optical properties of solid-state Br-TRZ under different stimuli-responsive conditions. The UV-Vis diffuse reflectance spectrum of pristine Br-TRZ presents one strong absorption peak below 400 nm region and the Br-TRZ powder is colorless, while the annealed Br-TRZ exhibits new absorption band at 400–500 nm (Figure S1, Supporting Information), which is derived from the more orderly

molecular arrangement. For emission spectra, Br-TRZ has an emission maximum at about 420 nm and shows intense blue fluorescence by 365 nm UV excitation. When the Br-TRZ material is annealed by heating, in contrast, not only does the emission spectrum show an emission at 420 nm, it also possesses a broad emission band from 500 to 650 nm with a maximum peak at 560 nm (Figure 2a). The time-correlated decay profile of Br-TRZ with annealing was also monitored at 420 and 560 nm, respectively (Figure S2 and Figure 2c). The emission decay at 420 nm belongs to a rapid nanosecond decay ( $\tau = 9.1$  ns), while the emission decay at 560 nm belongs to a microsecond-scale decay ( $\tau = 26.7$   $\mu$ s), indicating that the heat-induced long wavelength decay is RTP in nature. The phosphorescence quantum yield ( $\Phi_p$ ) was measured to be 3.10%. It is worth noting that such heat-induced RTP of Br-TRZ powders could be quenched through grinding process (Figure 2a), indicating the sensitivity of the organic RTP. According to previous works, this RTP should be originated from the ordered molecular packing induced by annealing.<sup>[41–43]</sup>

Figure 2b shows the photoluminescence emission spectra of the solids of Br-TRZ with TFA fuming and mechanical grinding. For the Br-TRZ solids with TFA fuming treatment, there are two signal peaks in emission spectrum: one at 395 nm, representing fluorescence, and the other one at 560 nm, representing phosphorescence, which is highly in accordance with that of annealed Br-TRZ. At the same time, it exhibits a strong RTP emission with a yellow color (inset photo in Figure 2b), and the  $\Phi_p$  also increases from nearly 0% to 3.29%. Furthermore, similar to the annealed Br-TRZ, the TFA treated Br-TRZ also exhibits an absorption band at 400–500 nm in UV-Vis diffuse reflectance spectrum (Figure S1). Protonation at the triazine site of Br-TRZ adds a positive charge and is likely to induce an obvious charge transfer state, which gives rise to the strong and red-shifted RTP compared to the vertical  $\pi$ - $\pi^*$  state.<sup>[44,45]</sup> It is worth mentioning that Br-TRZ still exhibits a detectable RTP at 520 nm with the treatment of grinding after TFA fuming (Figure 2b), with the  $\Phi_p = 1.49\%$ . These exciting results give us an impression that this kind of molecules as a model is much beneficial for the investigating

the mechanism of the unique RTP. Given the only difference between Br-TRZ and protonated Br-TRZ is the proton, it is reasonable to assume that the strong RTP is related to larger charge separation of the ground and/or excited state, or more pronounced charge transfer state. When analyzed with lifetime decay spectra, it was further confirmed that the 395 and 560 nm emission are attributed to the fluorescence and phosphorescence pathway (Figure S3 and Figure 2c). In other words, the reversible RTP switching on–off behavior was efficiently blocked by protonation effect, showing a specific “*Lock*” gate.

In a further set of powder X-ray diffraction (XRD) experiments, we investigated the influence of the different mode of molecular packing under various conditions (Figure 2d). In contrast with a few weaker and wider peaks of pristine dye molecules in XRD pattern, the TFA fuming Br-TRZ exhibit multiple highly sharp diffraction peaks at  $2\theta$  range from 5 to  $30^\circ$ , suggesting that the molecular stacking is transformed from disordered to ordered state.<sup>[46,47]</sup> After grinding the protonated materials, the sharp diffraction peaks disappeared and the wider peaks occurred again in XRD pattern, which demonstrates that the grinding breaks the ordered molecular packing to a great extent. By careful analysis of the emission spectrum of Br-TRZ with TFA fuming and mechanical grinding, we found that there is still a slight blue-shift RTP emission for Br-TRZ-H under “*Lock*” state and disordered molecular packing condition (Figure 2b), suggesting molecular packing has an effect on RTP character, but is not the decisive factor for RTP.

Interestingly, the RTP signal of protonated Br-TRZ could be quenched through fuming with TEA and the RTP could be recovered via TFA fuming, thus realizing a reversible RTP switching ON-OFF behavior (Figure 2e). Meanwhile, the reversible RTP ON-OFF character can be operated by acid-base pair (TFA and TEA), and the cycle process could be repeated for seven successive times, showing the excellent cycling stability (Figure 2f). These results indicate that TEA is considered as a “*Key*” to “*Lock*” (TFA) for RTP of Br-TRZ.

We expect that the nonbonding lone pair of nitrogen atom in Br-TRZ is a better binding site for TFA. To test our assumption, we performed  $^1\text{H}$  NMR measurements of Br-TRZ before and after stimulation with various molar ratios of TFA (Figure S4). We did not observe two sets of NMR peaks for Br-TRZ and H-Br-TRZ as anticipated; instead, all protons on Br-TRZ exhibit a gradual shift, but to different extents, to the downfield or upfield position after addition of TFA (Figure 3a). The doublet signals at 7.75, 7.62, and 7.55 ppm, which are indexed to  $\text{H}_b$ ,  $\text{H}_c$ , and  $\text{H}_d$ , are gradual shifted to downfield, demonstrating that after the addition of TFA, the electron density on triazine ring decrease and the formation of complex with proton. Furthermore, HRMS experiment of Br-TRZ with TFA was conducted to prove the complex of Br-TRZ with proton. As shown in Figure 3b, a signal peak at  $m/z$  771.9596 (measured exact mass) match well with the calculated mass of Br-TRZ with one proton. As expected, the typical quadruple isotope peaks of bromine located at ( $m/z$ ) 771.9596, 773.9576, 775.9558, and 777.9547 with intensity ratio 1:3:3:1 are observed, indicating the formation of complex Br-TRZ with one proton. Meanwhile, the peak of complex Br-TRZ with two, or three protons was not observed.

To probe the mechanism of the observed proton-gated RTP phenomenon from pure organic system, we performed theoretical calculation investigations on single-molecule Br-TRZ and Br-TRZ-H in both singlet and triplet excited states. The hole-electron distributions of Br-TRZ and Br-TRZ-H are depicted in Figure 4a and 4c. For Br-TRZ, the holes (blue area) are mainly distributed on the triazine cores and the electrons (yellow area) mainly distributed on the outside phenyl part. In contrast, For Br-TRZ-H, the holes are mainly distributed on the phenyl part and the electrons mainly distributed on the triazine cores, which is opposite to that of Br-TRZ. Meanwhile, the contributions of non-hydrogen atoms in Br-TRZ and Br-TRZ-H to hole, electron, and their overlap are shown in Figure 4b and 4d. Compared to Br-TRZ, protonated Br-TRZ-H exhibit more efficient electron-hole separation, demonstrating an intramolecular CT state in Br-TRZ-H that can bridge the energy gap between the lowest singlet and triplet

states. We also performed theoretical calculations to identify the energy gaps between the lowest singlet and triplet states for the neutral and protonated species. On the basis of data analysis, the calculated singlet–triplet energy gaps for Br-TRZ-H are 0.389 ( $S_1$ - $T_1$ ), 0.127 ( $S_1$ - $T_2$ ), 0.085 ( $S_1$ - $T_3$ ), and 0.026 eV ( $S_1$ - $T_4$ ), which is smaller than the corresponding energy gaps 0.441 ( $S_1$ - $T_1$ ), 0.212 ( $S_1$ - $T_2$ ), 0.103 ( $S_1$ - $T_3$ ), and 0.042 eV ( $S_1$ - $T_4$ ) for Br-TRZ (Figure 4e and Table S1). The calculated energy levels of Br-TRZ-H at the lowest singlet state ( $E_{S_1} = 2.83$  eV) and triplet ( $E_{T_1} = 2.44$  eV) excited states are close, which enhances the spin–orbit coupling probability and enables the facilitation of single–triplet intersystem crossing processes. These results prove that the key step for realizing gated RTP is the intramolecular charge transfer character that can narrow the singlet–triplet energy gap.

### 3. Conclusion

In summary, we have constructed a gated enhancement strategy controlled by complexation/dissociation with proton to achieve efficient RTP for organic luminogens. Solid state Br-TRZ show heat-induced RTP property, but the obtained RTP is easily quenched with the external mechanical force. Upon protonation, Br-TRZ-H species exhibit intense RTP emission at long wavelength region, and the strong RTP is still observed after grinding the Br-TRZ-H, realizing a proton-gated RTP. Theoretical calculations show that the protonation brings the enhanced intramolecular charge transfer, and sequentially resulting in the narrowed energy gap between the singlet and triplet states, finally leading to an efficient ISC process and thus stronger RTP. Furthermore, the gated RTP can be reversibly tuned *via* acid/base pair and show high fatigue resistance. The “*Lock/Unlock*” concept for the RTP property will provide an effective strategy for stabilizing the RTP emission of purely organic systems.

### Acknowledgements

This work was supported by the National Natural Science Foundation of China (22272109, 21908146, 21875143, 21700102, and 22002039), the Innovation Research Foundation of

Shenzhen (JCYJ20180507182229597), and the Foundation of Characterization Technique (Institute for Advanced Study, Central South University). Special thanks to the Instrumental Analysis of Shenzhen University (Lihu Campus). K. Gu, Z. Meng, X. W. Liu contributed equally to this work.

### Conflict of Interests

The authors declare no conflict of interests.

### Data Availability Statement (optional)

(Know more about the Wiley's Data Sharing Policies and provide the data availability statement according to the [Author Standard Template](#))

### Supporting Information

Supporting Information is available from the Wiley Online Library or from the author.

Received: ((will be filled in by the editorial staff))

Revised: ((will be filled in by the editorial staff))

Published online: ((will be filled in by the editorial staff))

### References

1. W. Zhao, Z. He, B. Z. Tang, *Nat. Rev. Mater.* **2020**, 5, 869.
2. J. Guo, C. Yang, Y. Zhao, *Acc. Chem. Res.* **2022**, 55, 1160.
3. R. Kabe, C. Adachi, *Nature* **2017**, 550, 384.
4. L. Gu, H. Shi, L. Bian, M. Gu, K. Ling, X. Wang, H. Ma, S. Cai, W. Ning, L. Fu, H. Wang, S. Wang, Y. Gao, W. Yao, F. Huo, Y. Tao, Z. An, X. Liu, W. Huang, *Nat. Photon.* **2019**, 13, 406.
5. S. M. A. Fateminia, Z. Mao, S. Xu, Z. Yang, Z. Chi, B. Liu, *Angew. Chem. Int. Ed.* **2017**, 56, 12160.
6. T. He, W. Guo, Y. Chen, X. Yang, C. Tung, L. Wu, *Aggregate* **2022**, 3, e250.



7. P. She, Y. Qin, Y. Ma, F. Li, J. Lu, P. Dai, H. Hu, X. Liu, S. Liu, W. Huang, Q. Zhao, *Sci. China Mater.* **2021**, *64*, 1485.
8. Q. Zhao, C. Huang, F. Li, *Chem. Soc. Rev.* **2011**, *40*, 2508.
9. Z. Pan, Y. Lu, F. Liu, *Nat. Mater.* **2012**, *11*, 58.
10. Y. Zhao, X. Yang, X. Lu, C. Yang, N. Fan, Z. Yang, L. Wang, L. Ma, *Inorg. Chem.* **2019**, *58*, 6215.
11. X. Wang, J. Gong, H. Zou, S. H. Liu, J. Zhang, *Aggregate* **2022**, *3*, e252.
12. X. Yu, K. Liu, H. Zhang, B. Wang, G. Yang, J. Li, J. Yu, *CCS Chem.* **2021**, *3*, 252.
13. X. Ma, J. Wang, H. Tian, *Acc. Chem. Res.* **2019**, *52*, 738.
14. J. Yang, M. Fang, Z. Li, *Aggregate* **2020**, *1*, 6.
15. Z. Mao, Z. Yang, Y. Mu, Y. Zhang, Y. Wang, Z. Chi, C. Lo, S. Liu, A. Lien, J. Xu, *Angew. Chem. Int. Ed.* **2015**, *54*, 6270.
16. X. Chen, C. Xu, T. Wang, C. Zhou, J. Du, Z. Wang, H. Xu, T. Xie, G. Bi, J. Jiang, X. Zhang, J. N. Demas, C. O. Trindle, Y. Luo, G. Zhang, *Angew. Chem. Int. Ed.* **2016**, *55*, 9872.
17. R. Liu, T. Jiang, D. Liu, X. Ma, *Sci. China Chem.* **2022**, *65*, 1100.
18. Z. He, H. Gao, S. Zhang, S. Zheng, Y. Wang, Z. Zhao, D. Ding, B. Yang, Y. Zhang, W. Z. Yuan, *Adv. Mater.* **2019**, *31*, 1807222.
19. O. Bolton, K. Lee, H. Kim, K. Y. Lin, J. Kim, *Nat. Chem.* **2011**, *3*, 205.
20. W. Z. Yuan, X. Y. Shen, H. Zhao, J. W. Y. Lam, L. Tang, P. Lu, C. Wang, Y. Liu, Z. Wang, Q. Zheng, J. Z. Sun, Y. Ma, B. Z. Tang, *J. Phys. Chem. C* **2010**, *114*, 6090.
21. Z. Yuan, J. Wang, L. Chen, L. Zou, X. Gong, X. Ma, *CCS Chem.* **2020**, *2*, 158.
22. S. Garain, S. N. Ansari, A. A. Kongasseri, B. Chandra Garain, S. K. Pati, S. J. George, *Chem. Sci.* **2022**, *13*, 10011.
23. H. E. Hackney, D. F. Perepichka, *Aggregate* **2022**, *3*, e123.

24. X. Zhang, L. Du, W. Zhao, Z. Zhao, Y. Xiong, X. He, P. F. Gao, P. Alam, C. Wang, Z. Li, J. Leng, J. Liu, C. Zhou, J. W. Y. Lam, D. L. Phillips, G. Zhang, B. Z. Tang, *Nat. Commun.* **2019**, *10*, 5161.
25. Z. Zhang, W. Xu, W. Xu, J. Niu, X. Sun, Y. Liu, *Angew. Chem. Int. Ed.* **2020**, *59*, 18748.
26. Y. Ning, J. Yang, H. Si, H. Wu, X. Zheng, A. Qin, B. Z. Tang, *Sci. China Chem.* **2021**, *64*, 739.
27. N. Gan, H. Shi, Z. An, W. Huang, *Adv. Funct. Mater.* **2018**, *28*, 1802657.
28. D. Lee, O. Bolton, B. C. Kim, J. H. Youk, S. Takayama, J. Kim, *J. Am. Chem. Soc.* **2013**, *135*, 6325.
29. L. Gu, H. Wu, H. Ma, W. Ye, W. Jia, H. Wang, H. Chen, N. Zhang, D. Wang, C. Qian, Z. An, W. Huang, Y. Zhao, *Nat. Commun.* **2020**, *11*, 944.
30. Z. An, C. Zheng, Y. Tao, R. Chen, H. Shi, T. Chen, Z. Wang, H. Li, R. Deng, X. Liu, W. Huang, *Nat. Mater.* **2015**, *14*, 685.
31. Q. Li, M. Zhou, M. Yang, Q. Yang, Z. Zhang, J. Shi, *Nat. Commun.* **2018**, *9*, 734.
32. L. Bian, H. Shi, X. Wang, K. Ling, H. Ma, M. Li, Z. Cheng, C. Ma, S. Cai, Q. Wu, N. Gan, X. Xu, Z. An, W. Huang, *J. Am. Chem. Soc.* **2018**, *140*, 10734.
33. J. Yang, M. Fang, Z. Li, *Acc. Mater. Res.* **2021**, *2*, 644.
34. H. Li, H. Li, W. Wang, Y. Tao, S. Wang, Q. Yang, Y. Jiang, C. Zheng, W. Huang, R. Chen, *Angew. Chem. Int. Ed.* **2020**, *59*, 4756.
35. Y. Wang, J. Yang, M. Fang, Y. Yu, B. Zou, L. Wang, Y. Tian, J. Cheng, B. Z. Tang, Z. Li, *Matter* **2020**, *3*, 449.
36. Y. Mu, Z. Yang, J. Chen, Z. Yang, W. Li, X. Tan, Z. Mao, T. Yu, J. Zhao, S. Zheng, S. Liu, Y. Zhang, Z. Chi, J. Xu, M. P. Aldred, *Chem. Sci.* **2018**, *9*, 3782.
37. Y. Tani, M. Komura, T. Ogawa, *Chem. Commun.* **2020**, *56*, 6810.
38. Y. Liu, Z. Ma, X. Cheng, C. Qian, J. Liu, X. Zhang, M. Chen, X. Jia, Z. Ma, *J. Mater. Chem. C* **2021**, *9*, 5227.

39. R. Berger, J. Hauser, G. Labat, E. Weber, J. Hulliger, *CrystEngComm* **2012**, *14*, 768.
40. X. W. Liu, W. Zhao, Y. Wu, Z. Meng, Z. He, X. Qi, Y. Ren, Z. Yu, B. Z. Tang, *Nat. Commun.* **2022**, *13*, 3887.
41. Q. Li, Z. Li, *Acc. Chem. Res.* **2020**, *53*, 962.
42. J. Yang, X. Zhen, B. Wang, X. Gao, Z. Ren, J. Wang, Y. Xie, J. Li, Q. Peng, K. Pu, Z. Li, *Nat. Commun.* **2018**, *9*, 840.
43. Y. Wang, J. Yang, Y. Tian, M. Fang, Q. Liao, L. Wang, W. Hu, B. Z. Tang, Z. Li, *Chem. Sci.* **2020**, *11*, 833.
44. W. Sun, Z. Wang, T. Wang, L. Yang, J. Jiang, X. Zhang, Y. Luo, G. Zhang, *J. Phys. Chem. A* **2017**, *121*, 4225.
45. H. Han, E. Kim, *Chem. Mater.* **2019**, *31*, 6925.
46. Y. Xie, Y. Ge, Q. Peng, C. Li, Q. Li, Z. Li, *Adv. Mater.* **2017**, *29*, 1606829.
47. S. Li, Y. Xie, A. Li, X. Li, W. Che, J. Wang, H. Shi, Z. Li, *Sci. China Mater.* **2021**, *64*, 2813.

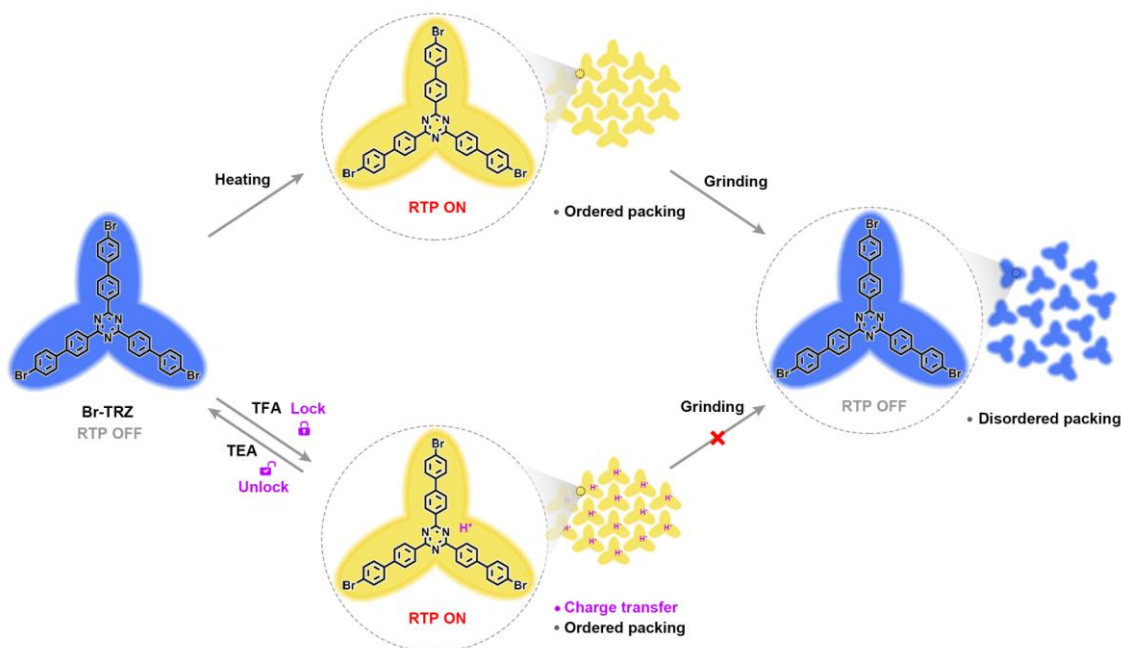


**Figure 1.** Schematic illustration of the proton-gated RTP strategy for stabilizing room-temperature phosphorescence of pure organic molecules.

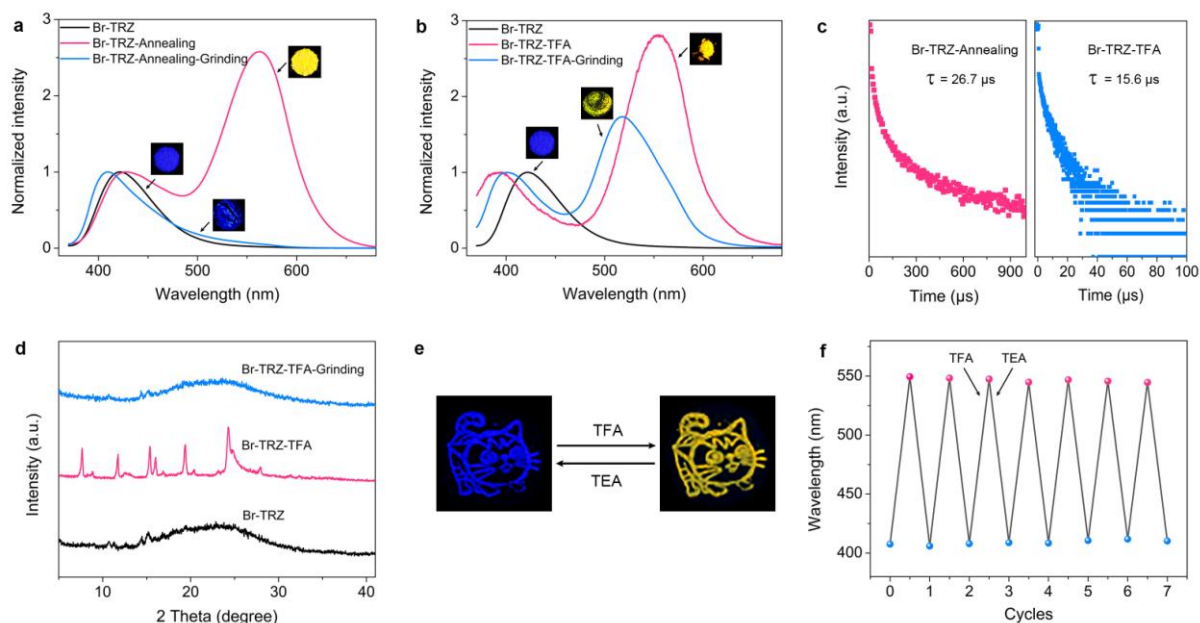


**Figure 2.** Proton-gated RTP investigating by spectroscopic characterizations. Emission spectra of solid state Br-TRZ with (a) annealing/grinding and (b) TFA fuming/grinding. (c) The time-resolved decay curves of Br-TRZ with annealing or TFA fuming at 560 nm,  $\lambda_{\text{ex}} = 350$  nm. (d) XRD spectra of Br-TRZ with TFA fuming/grinding. (e) Photos showing photoluminescence of Br-TRZ with TFA and TEA fuming. (f) Cycling stability of Br-TRZ with TFA and TEA fuming in a "Lock-and-Unlock" manner.

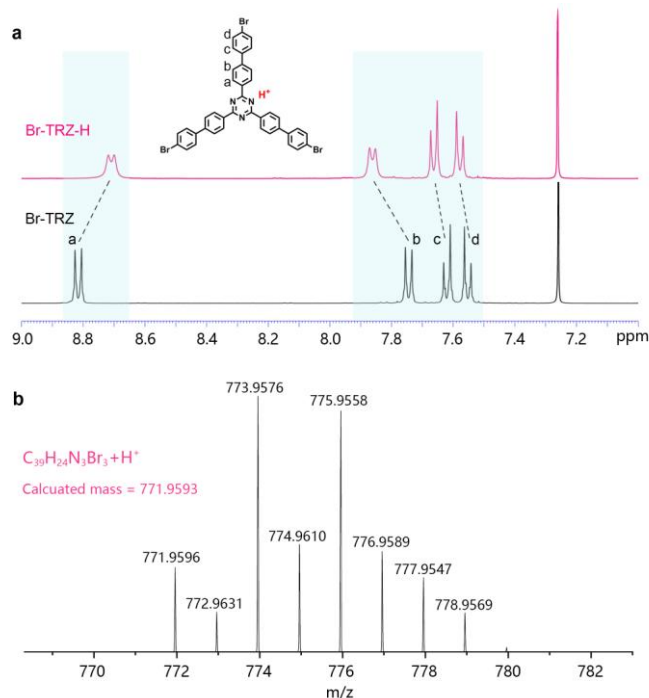


**Figure 3.** Characterization of the protonated Br-TRZ with one proton. (a)  $^1\text{H}$  NMR spectra of Br-TRZ (5  $\mu\text{M}$ ) and Br-TRZ in the presence of TFA (40 equiv.) in  $\text{CDCl}_3$ . (b) HRMS spectra of Br-TRZ in the presence of TFA.

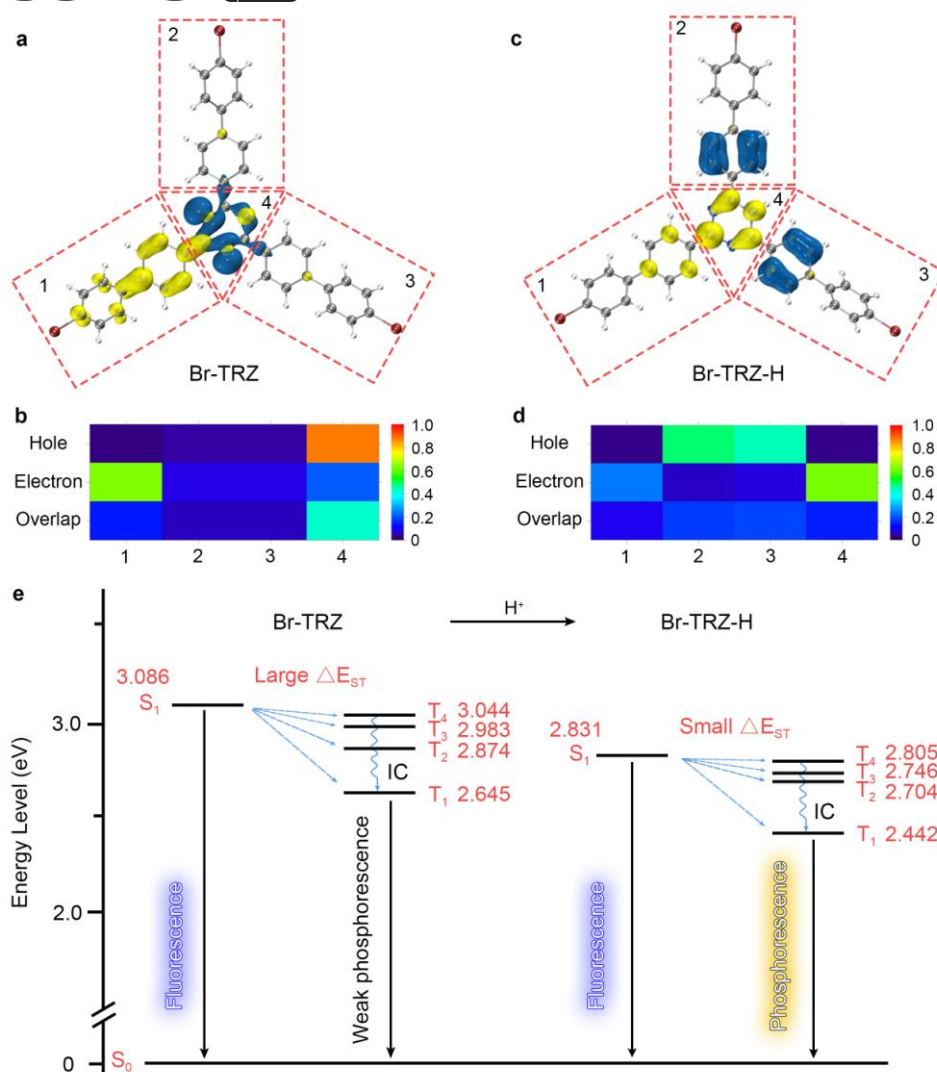


**Figure 4.** Theoretical calculation for fluorescence and RTP behaviors of Br-TRZ and Br-TRZ-H. Electron and hole distributions of  $S \rightarrow T$ , and contribution of moiety to holes, electrons and hole/electron overlap of (a and b) Br-TRZ and (c and d) Br-TRZ-H (yellow represents electron distribution; blue represents hole distribution). (e) Calculated energy diagram of  $S_1$  and  $T_n$  of Br-TRZ and Br-TRZ-H.

By enhancing the intramolecular charge transfer effect of bromine-substituted triazine derivative (Br-TRZ), the protonated Br-TRZ stubbornly possesses a robust RTP under external stimulus, whatever in the ordered or disordered intermolecular arrangement state.

**Keywords:** room-temperature phosphorescence, gated effect, grinding, protonation, molecular packing

Kaizhi Gu, Zhengong Meng, Xing Wang Liu, Yue Wu,\* Xin Qi, Yiran Ren, Zhen-Qiang Yu,\* and Ben Zhong Tang\*

## A gated strategy stabilizes room-temperature phosphorescence

TOC figure

